Probabilistic Transient Stability Constrained Optimal Power Flow for Power Systems with Multiple Correlated Uncertain Wind Generations

S. W. Xia, *Student Member,* X. Luo, K. W. Chan, *Member, IEEE,* M. Zhou, and G.Y. Li

***Abstract*—This paper proposes a novel probabilistic transient stability constrained optimal power flow (P-TSCOPF) model to simultaneously consider uncertainties and transient stability for power system preventive control. While detailed wind generator model with rotor flux magnitude and angle control strategy is used to describe the dynamic behaviors of wind generators, uncertain factors with correlations, such as probabilistic load injections, stochastic fault clearing time and multiple correlated wind generations, are also included to form a representative P-TSCOPF model. A new GSO-PE approach, consisting of an improved group search optimization (GSO) and 2*m*+1 point estimated (PE) method with Cholesky decomposition, is then designed to effectively solve this challenging P-TSCOPF problem. The proposed P-TSCOPF model and GSO-PE solution approach have been thoroughly tested on a modified New England 39-bus system with correlated uncertain wind generations. Comparative results with Monte Carlo (MC) simulations have confirmed the validity of the P-TSCOPF model and demonstrated the effectiveness of GSO-PE method.**

***Index Terms*—Probabilistic transient stability, Optimal power flow, Uncertainties, Correlated wind power, Point estimated method, Improved group search optimization.**

I. INTRODUCTION

Worldwide increasing concerns on the depletion of fossil energy resources and their environmental effects have driven the rapid development of green and sustainable renewable generations in power systems, while their inherent intermittences lead to high-level uncertainties and bring new challenges for power systems as well. The effects of these uncertainties on system operation and control need to be thoroughly analyzed and investigated by probabilistic studies for both static and dynamic security.

Existing papers mainly focus on the probabilistic static security analysis of power systems by probabilistic power flow [1-3] or probabilistic optimal power flow [4-7]. Given a probabilistic model of uncertain load demands or renewable power generations, the mean and standard deviations of concerned outputs such as bus voltages and line flows are quantified and the static security risk for power system operation is then analyzed. Papers dealing with the effects of renewables' uncertainties on the probabilistic dynamic security of power systems are less common, with only the traditional uncertainties such as uncertain loads, probabilistic fault occurrence, location, type and clearing time studied mainly by the probabilistic transient stability analysis (PTSA). The basic theory of PTSA was preliminarily reported in [8, 9], and then further investigated in [10]. While previous PTSA was based on the regression of critical clearing time in terms of system load distribution [11-13], recent PTSA is conducted using Monte Carlo (MC) method and conditional probability theory [14-16]. Most notably, a probabilistic-based approach was presented in [17] to evaluate the probabilistic transient stability of a wind farm with two-mass shaft wind turbines using EMTP.

Though MC method is straightforward, accurate and well-tested, it is very time consuming for PTSA as a large number of random time domain simulations are needed to determine the probabilistic transient stability index. As an alternative, the analytical method, which handles uncertainties based on linearization and obtains the probability of random output variables using convolution or comulant strategies, could be more computationally efficient though some mathematical assumptions are required to simplify the relationship between the concerned outputs and uncertain inputs. Since the linearization between the output state variables and inputs could be conveniently obtained from the Jacobian matrix in power flow calculation, this method was readily applied in probabilistic power flow for probabilistic static security analysis [18, 19]. Nevertheless, this approach would still be arduous for PTSA as linearizing the transient stability index in terms of the uncertain inputs, say by trajectory sensitivities, is by itself a challenge for practical power systems with a large number of complicated dynamic components.

So far, the current state-of-the-art PTSA is conducted mostly for power systems with uncertain parameters. The effects of uncertain renewables and how to further effectively and economically improve the system probabilistic transient security (risk) level are still not fully addressed yet. A new optimal model aiming to enhance the system probabilistic transient security at an economic cost would be timely needed for a new generation of power system preventive control. As a consequence, a new probabilistic transient stability constrained optimal power flow (P-TSCOPF) model which also considers stochastic load injections, fault clearing time, and correlated wind generations with a doubly fed induction generator (DFIG) dynamic models is proposed in this paper.

However, considering that PTSA alone is already complex and time-consuming, the new P-TSCOPF model which embeds PTSA in an optimization for probabilistic transient stability enhancement would be even more computational demanding and time-consuming. How this optimal model could be efficiently solved is crucial to the practical utilization of P-TSCOPF model in power industries. As a remedy, a new efficient GSO-PE solution approach is developed to effectively solve this P-TSCOPF problem based on an improved group search optimization (GSO) and 2*m*+1 PE method with Cholesky decomposition [20, 21]. In this paper, the proposed P-TSCOPF model and GSO-PE approach are thoroughly tested and evaluated using a modified New England system.

This work was supported in part by The Hong Kong Polytechnic University under Project G-UA3Z, National Natural Science Foundation of China (51190103), and PhD studentships awarded to S. W. Xia and X. Luo.

S. W. Xia, M. Zhou and G.Y Li are with State Key Laboratory of Alternate Electrical Power System with Renewable Energy Sources, North China Electric Power University, Beijing 102206, China (e-mail: s.w.xia@ncepu.edu.cn; zhouming@ncepu.edu.cn; ligy@ncepu.edu.cn).

X. Luo and K. W. Chan are with the Department of Electrical Engineering, The Hong Kong Polytechnic University, Hong Kong SAR, China (e-mail: luo.xiao.peter@connect.polyu.hk; eekwchan@ polyu.edu.hk).

The following publication S. Xia, X. Luo, K. W. Chan, M. Zhou and G. Li, "Probabilistic Transient Stability Constrained Optimal Power Flow for Power Systems With Multiple Correlated Uncertain Wind Generations," in IEEE Transactions on Sustainable Energy, vol. 7, no. 3, pp. 1133-1144, July 2016 is available at https://doi.org/10.1109/TSTE.2016.2520481.

In deregulated power systems, independent grid operators would employ security constrained economic dispatch (SCED) and security constrained unit commitment (SCUC) to clear real time and day-ahead markets. Generally, SCED and SCUC could effectively minimize the system operating cost without violating any static generator output limits, AC network transmission line limits, nodal voltage limits, etc. [22-24]. Though static security requirements could be ensured by SCED and SCUC, many power systems around the world are stressed and prone to transient instability [25-28]. Compared with SCED and SCUC, the proposed P-TSCOPF model is capable of reconciling economics, transient stability and uncertainties of renewables simultaneously and could potentially be used to replace the conventional SCED for real time market clearing and further developed as an advanced day-ahead generation commitment tool with consideration of uncertainties and dynamic stability.

The main contributions of this paper include: 1) an original P-TSCOPF model simultaneously considering uncertain factors, transient stability and economic is presented for power system preventive control; 2) apart from the conventional uncertain factors such as load demand and fault clearing time, the correlated uncertain wind generations with its dynamic generator model are included in P-TSCOPF; 3) the newly proposed GSO-PE approach could efficiently solve the P-TSCOPF model and effectively enhance the system probabilistic transient stability level when benchmarked on the New England system with multiple wind farms; 4) the proposed P-TSCOPF model and GSO-PE method are general and flexible to support any other types of uncertain renewables and dynamic models**.**

The rest of this paper is organized as follows. A general P-TSCOPF model is first proposed in Section II, and then a specific P-TSCOPF model with uncertain load injections, wind generation and fault clearing time is presented in Section III. In Section IV, the GSO-PE algorithm is formed to solve the P-TSCOPF model, and Section V validates this method on a modified New England system. Conclusions and future work are given in the last Section.

II. General Form of Proposed P-TSCOPF Model

The proposed P-TSCOPF model is mathematically formulated as

$$\text{Minimize} \quad E\{F(\mathbf{x}^{t_0},\mathbf{y}^{t_0},\mathbf{u},\boldsymbol{\varepsilon})\} \tag{1}$$

$$\text{Subject to} \quad \mathbf{G}(\mathbf{x}^{t_0},\mathbf{y}^{t_0},\mathbf{u},\boldsymbol{\varepsilon})=0 \tag{2}$$

$$P\{h_j(\mathbf{x}^{t_0},\mathbf{y}^{t_0},\mathbf{u},\boldsymbol{\varepsilon})\le \mathbf{0}\}\ge \beta_j \tag{3}$$

$$\begin{cases} \dfrac{d\mathbf{x}}{dt}=\mathbf{H}(\mathbf{x}(t),\mathbf{y}(t),\mathbf{u},\boldsymbol{\varepsilon}) \\ \mathbf{G}(\mathbf{x}(t),\mathbf{y}(t),\mathbf{u},\boldsymbol{\varepsilon})=0 \quad t\in(t_0,t_{end}] \\ \mathbf{x}(t_0)=\mathbf{x}^{t_0},\mathbf{y}(t_0)=\mathbf{y}^{t_0} \end{cases} \tag{4}$$

$$P\{\eta(\mathbf{x}(t),\mathbf{y}(t),\mathbf{u},\boldsymbol{\varepsilon})>0\}\ge\beta_r \tag{5}$$

where $E\{\}$ stands for the expectation calculation; $\boldsymbol{\varepsilon}$ are the uncertain variables; $\boldsymbol{u}$ are the control variables with lower and upper limits, such as the generator active power and terminal voltage; $\mathbf{x}(t)$ and $\mathbf{y}(t)$ are the state and algebraic variables during the transient period $(t_0, t_{end}]$ with initial values $\mathbf{x}^{t_0}$ and $\mathbf{y}^{t_0}$; at starting time t_0 ; η is the transient stability margin. Since the objective function would depend on the uncertain variables, its expectation is adopted as the P-TSCOPF objective in (1). (2) stands for steady-state power flow equation. (3) requires the chance constraints for steady-state variables, such as nodal voltage magnitudes and transmission line thermal limits, above a fixed risk security level β_j. (4) describes the dynamics of the power system during the transient period, including complex generator models with AVR and renewable generation dynamic models. (5) is the probabilistic transient stability constraint with an acceptable security level β_r.

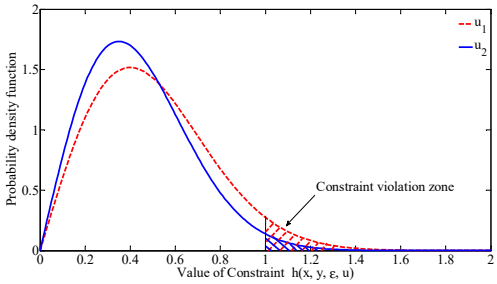

Fig. 1 Constraint violations for different control variables

Fig. 1 simply shows the idea of P-TSCOPF model. The probabilistic constraint $h(\boldsymbol{x},\boldsymbol{y},\boldsymbol{\varepsilon},\boldsymbol{u})$ or $\eta(\boldsymbol{x},\boldsymbol{y},\boldsymbol{\varepsilon},\boldsymbol{u})$ has two violation risk levels for different control variables $\boldsymbol{u}_1$ and $\boldsymbol{u}_2$ with diverse objective expectation $E\{f(\boldsymbol{x},\boldsymbol{y},\boldsymbol{\varepsilon},\boldsymbol{u})\}$. For example, the constraint violation probability for $\boldsymbol{u}_1$ is larger than $\boldsymbol{u}_2$ in Fig.1 while their expected objectives are different. As the compromise for smaller probability of constraints violation, the proposed P-TSCOPF would be solved for the best control $\boldsymbol{u}$ with minimal expected objective value above a satisfactory security level.

III.P-TSCOPF Problem: Explicit Formulation

While the general form of P-TSCOPF model is presented in Section II, here a representative P-TSCOPF model used in the case study is explicitly given with brief descriptions on how various uncertain variables could be considered in P-TSCOPF.

A. Uncertainties considered in the proposed model

For simplicity, only the following three uncertain variables: load injections, wind generations, and fault clearing time, are considered for a given deterministic contingency in this paper, while other common contingency related uncertain factors, such as probabilistic fault occurrence, fault type and location, could be easily tackled using the conditional probability approach based on the discrete probabilistic models in [15, 16].

1) Probabilistic model of load injections

The continuous varying load injections are important sources of uncertainties in practical power systems. As commonly used in probabilistic power flow analysis [29-31] and PTSA [11, 12, 32-34], the normal distribution (6) is adopted here to describe the uncertainty of active load injection P_{Di}

$$f(P_{D_i})=\frac{1}{\sqrt{2\pi}\sigma_p}e^{-(P_{D_i}-\mu_p)^2/2\sigma_p^2} \tag{6}$$

where σ_p and μ_p are the mean and standard deviation of probabilistic load active power. Often power consumptions at different buses have related patterns due to meteorological and social factors; for instance, power demands for some buses are higher in holiday, evening or in cold days. It has been reported that the dependences of load demands at different buses have a considerable effects on the probabilistic results and shall be

considered in probabilistic assessment [29-31]. As in [29-31], the dependences of active load injections at different locations are represented by the correlation coefficients C_{pd} in this paper. The reactive load injection Q_{Di} is modeled as a variable with a constant ratio to its corresponding active load.

2) Probabilistic model of wind generations

The popular Weibull distribution with shape parameter λ and scale parameter k is used for modeling the probabilistic wind speed v_w [35] as follows

$$f(v_w,\lambda,k)=\frac{k}{\lambda}(\frac{v_w}{\lambda})^{k-1}e^{-(\frac{v_w}{\lambda})^k} \tag{7}$$

While wind speeds at sites far apart from each other could be assumed independent, many wind sites are geographically close. For generality, correlations of wind speeds at different locations should be considered for power system probabilistic analysis [1, 36-38]. The correlation coefficient with a range [-1, 1], denoted as C_v in this paper, is an effective parameter to quantify how well wind speeds at two sites follow each other. In specific, if the C_v is positive, wind speeds at two sites change in the same direction, vs in opposite direction for negative C_v. If C_v is zero, the wind speeds at two sites are uncorrelated, or they do not follow each other.

With probabilistic wind speed, a wind generator output is determined from the speed-power curve of wind turbine [35].

$$P_m=\begin{cases}0, & (v_w<v_{ci},\ v_w>v_{ct})\\ P_{rated}\cdot(\dfrac{v_w-v_{ci}}{v_{rd}-v_{ci}}), & (v_{ci}\le v_w\le v_{rd})\\ P_{rated}, & (v_{rd}<v_w<v_{ct})\end{cases} \tag{8}$$

where P_{rated} is the rated power; v_{ci}, v_{rd} and v_{ct} are the cut-in, rated and cut-out wind speed, respectively. The distribution of wind generations can be calculated from (8) using the wind speed samples based on its probabilistic model (7).

3) Probabilistic model of fault clearing time

The fault clearing time t_{cl}, associated with the protection device to detect and remove fault from power systems, is an important uncertain factor for PTSA. According to the investigations in [9, 14, 16, 17], a widely used normal distribution probabilistic model is adopted here for the fault clearing time.

$$f(t_{cl})=\frac{1}{\sqrt{2\pi}\sigma_t}e^{-(t_{cl}-\mu_t)^2/2\sigma_t^2} \tag{9}$$

where μ_t and σ_t are mean and standard deviations of t_{cl}.

B. Explicit formulation of Proposed P-TSCOPF

With the uncertainties represented as above, the P-TSCOPF model can be explicitly formulated as follows.

1) Objective function

Usually, slack bus generator is used to keep the power balance in the system. However, the uncertainties of random input variables would cause the slack bus generation become probabilistic. Therefore, the system state variables and concerned objectives will be probabilistic too. In this paper, the expected total generation fuel cost is adopted as the objective of the P-TSCOPF model

$$F_G=E\{\sum_{i=1}^{n_G}(a_iP_{Gi}^2+b_iP_{Gi}+c_i)\} \tag{10}$$

where P_{Gi} is active power of the ith generator and n_G is total number of traditional generators. It shall be noted that there is no limitation on the formulation of the P-TSCOPF objective, and many other targets, such as expected minimum power loss, expected participants' bids in power market, could be similarly designed as the objective of P-TSCOPF or even extended to form a multiple-objective P-TSCOPF model.

The static equality constraint (2) is explicitly described by the power flow equations as

$$\begin{cases}0=P_{Gi}+P_w-P_{Di}-V_i\sum_{j=1}^{n_b}V_j(G_{ij}\cos\theta_{ij}+B_{ij}\sin\theta_{ij})\\ 0=Q_{Gi}+Q_w-Q_{Di}-V_i\sum_{j=1}^{n_b}V_j(G_{ij}\sin\theta_{ij}-B_{ij}\cos\theta_{ij})\end{cases} \tag{11}$$

where i=1,2,…,n_b; n_b is the total number of nodes; Q_{Gi} and Q_{Di} are the generator and load reactive power; V_i and V_j are the voltage magnitude of node i and j; θ_{ij} is the angle difference between node i and j. These active and reactive power balance constraints are enforced in initialization and subsequent time domain simulations for transient stability analysis.

2) Static probabilistic inequality constraints

The static inequality constraint (3) explicitly includes the probabilistic constraints for generator reactive power, node voltage and transmission line thermal limits as (12)-(14)

$$P\{Q_{Gi\min}\le Q_{Gi}\le Q_{Gi\max}\}>\beta_Q\quad(i=1,2,.....,n_G) \tag{12}$$

$$P\{V_{i\min}\le V_i\le V_{i\max}\}>\beta_V\quad(i=1,2,.....,n_b) \tag{13}$$

$$P\{S_{l_i}\le S_{l_i\max}\}>\beta_S\quad(i=1,2,.....n_l) \tag{14}$$

where n_l is the number of branches and S_{li} is the apparent power flow in the ith branch; $Q_{Gi\min}$, $Q_{Gi\max}$, $V_{Gi\min}$ and $V_{Gi\max}$ are the lower and upper limits of generator reactive power and bus voltage, respectively; S_{limax} is upper limit of the ith transmission line power. These probabilistic constraints ensure that bus voltages, generator reactive powers and transmission line power flows are all bounded in the required ranges with an acceptable risk security level.

3) Dynamic equality constraint

Equality constrains (4) are a set of differential algebraic equations (DAEs) describing the behaviors of power system dynamic components including traditional and wind generator systems. In this paper, a fourth-order dynamic model with IEEE Type 1 exciter [39] is adopted for representing the traditional generators, while the dynamic wind generator system consists of a two lumped-mass shaft wind turbine (WT) model as described in (15)-(16) and a doubly fed induction generator (DFIG) model shown in Fig. 2.

$$\frac{\mathrm{d}\theta_{\mathrm{tw}}}{\mathrm{d}t}=\omega_{\mathrm{s}}\left(\omega_{\mathrm{t}}-\omega_{\mathrm{r}}\right) \tag{15}$$

$$\frac{\mathrm{d}\omega_{\mathrm{t}}}{\mathrm{d}t}=\frac{1}{2H_{\mathrm{t}}}\left[\frac{P_m}{\omega_{\mathrm{t}}}-K_{\mathrm{tw}}\theta_{\mathrm{tw}}-D_{\mathrm{tw}}\left(\omega_{\mathrm{t}}-\omega_{\mathrm{r}}\right)\right] \tag{16}$$

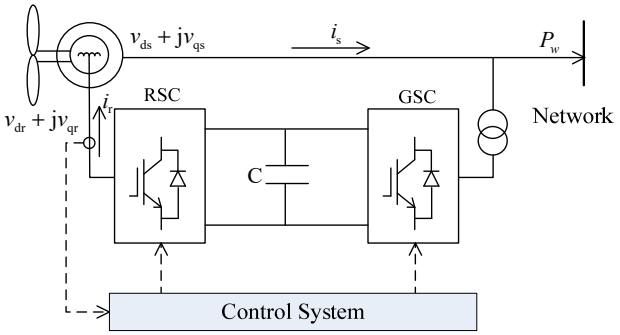

Fig. 2 DFIG structure

where ω_t, ω_r and ω_s are the turbine speed, rotor speed and system synchronous speed, respectively; θ_{tw} (rad) is the shaft twist angle; K_{tw} (p.u./rad) and D_{tw} are the shaft stiffness and mechanical damping coefficients; H_t (s) is wind turbine inertia constant; P_m is the mechanical power extracted from the wind.

By ignoring the dynamics of stator currents, the widely used third order DFIG for stability analysis is derived as [40]

$$\frac{1}{\omega_b}\frac{de_d}{dt} = -\frac{1}{T_0}\left[e_d - (X - X')i_{qs}\right] + s\omega_s e_q - \omega_s \frac{L_m}{L_r + L_m} v_{qr} \quad (17)$$

$$\frac{1}{\omega_b}\frac{de_q}{dt} = -\frac{1}{T_0}\left[e_q + (X - X')i_{ds}\right] - s\omega_s e_d + \omega_s \frac{L_m}{L_r + L_m} v_{dr} \quad (18)$$

$$\frac{d\omega_r}{dt} = \frac{1}{2H_g}\left[K_{tw}\theta_{tw} + D_{tw}(\omega_t - \omega_r) - (e_d i_{ds} + e_q i_{qs})\right] \quad (19)$$

$$v_{ds} = -r_s i_{ds} + X' i_{qs} + e_d \quad (20)$$

$$v_{qs} = -r_s i_{qs} - X' i_{ds} + e_q \quad (21)$$

$$P_w = v_{ds} i_{ds} + v_{qs} i_{qs} - v_{dr} i_{dr} - v_{qr} i_{qr} \quad (22)$$

$$Q_w = v_{qs} i_{ds} - v_{ds} i_{qs} \quad (23)$$

where e_d , e_q , v_{ds}, v_{qs} , v_{dr} and v_{qr} are, respectively, d and q components of the internal voltage, stator voltage and rotor voltage; i_{ds} , i_{qs} , i_{dr} and i_{qr} are d and q components of stator and rotor current; P_w and Q_w are the output active and reactive power of DFIG; r_s is stator resistance; X and X' are the open-circuit and short-circuit reactance; T_0 is the transient open-circuit time constant; and H_g is the generator inertia constant. The control system of DFIG adopts a FMAC structure with two control loops as shown in Fig. 3 [40], one for the terminal voltage and the other for the power output of DFIG with the advantages of (1) providing low interaction between the power and voltage control loop, and (2) enhancing voltage recovery after faults. In Fig. 3, the power output reference is derived from the rotor speed w_r via a maximum power extraction characteristic lookup table.

4) Probabilistic transient stability constraint

The SIngle Machine Equivalent (SIME) method is an effective hybrid temporal-direct algorithm for multi-machine systems transient stability analysis. It uses time domain simulation results to (1) observe systems stability in a SIME frame by examining the equivalent critical machine (CM) and non-critical machine (NM), and then (2) determine the stability margin according to equal-area criterion [41-43]. Since it is a time simulation based method, SIME is capable to conduct transient stability analysis for power systems with any complex models, such as generators with AVR-Governor-PSS or DFIG models. Since SIME has been widely used for transient stability assessment in practical systems [41-43] and TSCOPF problem [44, 45], it is adopted in this paper for conducting the transient stability analysis. Following the SIME theory with machines separated into CMs and NMs, the original system can be mapped into

$$\begin{cases} M_E \dfrac{d\omega_E}{dt} = P_{mE} - P_{eE} \\ \dfrac{d\delta_E}{dt} = \omega_E \end{cases} \quad (24)$$

where $M_E = M_C M_N / (M_C + M_N)$ stands for the equivalent inertial coefficient in one-machine infinite bus (OMIB), and subscripts 'C' and 'N' stand for CM and NM; $\delta_E = \delta_C - \delta_N$ and $\omega_E = \omega_C - \omega_N$ are the OMIB angle and speed. The mechanical power and electric power are $P_{mE} = M_E(M_C^{-1}P_{mC} - M_N^{-1}P_{mN})$ and $P_{eE} = M_E(M_C^{-1}P_{eC} - M_N^{-1}P_{eN})$, respectively.

For an unstable case, the stability margin is calculated as the residual dynamic energy at the time to instability t_u [44, 45], when its electrical power curve meets the mechanical power curve under the instability conditions (26).

$$\eta = -\frac{1}{2}M_E(\omega_E(t_u))^2 \quad (25)$$

$$\begin{cases} P_a(t_u) = P_{mE}(t_u) - P_{eE}(t_u) = 0 \\ \dot{P}_a(t_u) = \dfrac{dP_a}{dt} > 0 \end{cases} \quad (26)$$

For a stable case, the system stops its excursion at δ_r and returns for the reverse swing. The stability margin is

$$\eta = -\int_{\delta_r}^{\delta_u} P_a d\delta = \int_{\delta_r}^{\delta_u} |P_a| d\delta \quad (27)$$

where δ_u is the angle at the moment when the generator active power crosses mechanical for the less unstable case [43-45], and δ_r is the return angle at returning moment t_r when the system satisfies

$$\begin{cases} \omega(t_r) = 0 \\ P_a(t_r) < 0 \end{cases} \quad (28)$$

With stability margin η calculated by (25) and (27), the probabilistic stability constraint (5) is expressed as

$$P\{\eta > 0\} \geq \beta_r \quad (29)$$

In other words, the proposed explicit P-TSCOPF model would consist of objective (10), power balance equality constraint (11), DAEs for the wind generator model (15)-(23) and four-order traditional generators with IEEE Type 1 exciters, probabilistic static inequality constraints (12)-(14), and probabilistic transient stability constraints (29). The challenge for solving this model is how the probabilistic constraints (12)-(14) and (29) could be effectively evaluated.

IV. Methodology

The new GSO-PE method proposed here uses a two-stage approach for solving the P-TSCOPF model. In the first stage, the PE method is used to transform the PTSA into a set of deterministic transient stability analysis process and afterwards calculate the probability of concerned outputs (corresponding to step (6) to (8) in Fig.4, Section IV). An improved GSO

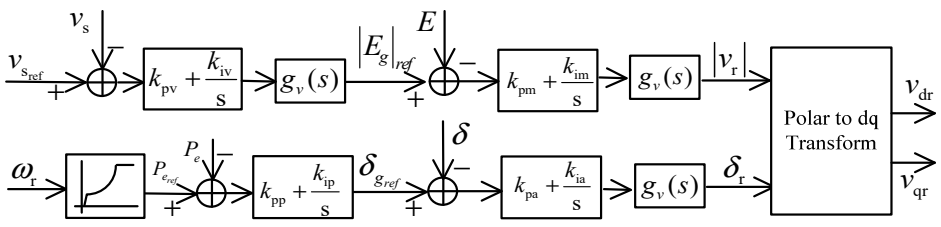

Fig. 3 Block diagram of FMAC controller

algorithm is then used in the second stage (corresponding to step (5) and (9)-(11) in Fig. 4) to search for the optimal control variables that would minimize the expected total fuel cost as well as satisfy all the probabilistic security constraints.

A. Point estimated method with Cholesky decomposition

The PE method is a promising and efficient tool for handling probabilistic problems, since it is capable of calculating the raw moments of output random variables from the deterministic solutions of only a few samples compared to numerous samples required in MC. Among the PE variants such as 2m and 4m+1 schemes, 2m+1 PE has been found to provide the best performance with satisfactory accuracy of results at the cost of relatively low computational burden **[20, 21]**. This paper will therefore introduce the 2m+1 PE method with Cholesky decomposition strategy to deal with the correlated uncertainties in the P-TSCOPF model.

The core of 2m+1 PE method is to generate three typical samples (named as concentrations of PE) for each uncertain variable in the condition that these three samples should retain the statistical information of the original uncertain variable [20, 21]. Based on these samples and the function relating input and output variables, the uncertainty properties of output variables can be estimated.

In the proposed model, the uncertain input variables include stochastic load injections, uncertain wind generations and the normal distributed fault clearing time, which can be denoted in an uncertain vector (z_1 , z_2 ,..., z_l ,... ,z_m) with m dimensions. Based on probability theory [20, 21], PE method would generate 2m+1 concentrations for this uncertain vector as follows.

1) Generate three concentrations for uncertain element z_l: the uncertain element z_l is replaced with three locations $z_{l,k}$ (k=1,2,3) while the remaining m-1 uncertain elements are fixed at their mean value μ_{z1}, μ_{z2},..., $\mu_{z(l-1)}$, $\mu_{z(l+1)}$, ..., μ_{zm}, thus three vectors would be generated in terms of (μ_{z1} , μ_{z2},..., $\mu_{z(l-1)}$, $z_{l,k}$, $\mu_{z(l+1)}$,..., μ_{zm}) (k=1,2,3) as three concentrations.
2) Repeat procedure (*1)* for each element of the uncertain vector (z_1 , z_2 ,..., z_l ,... ,z_m), and with m random elements, in total 3m concentrations (μ_{z1} , μ_{z2},..., $\mu_{z(l-1)}$, $z_{l,k}$, $\mu_{z(l+1)}$,..., μ_{zm}) (k=1,2,3, l=1,2,…,m) would be produced.

The location $z_{l,k}$ is calculated as

$$z_{l,k} = \mu_{zl} + \varepsilon_{l,k} \cdot \sigma_{zl} \quad k = 1,2,3 \tag{30}$$

where $\varepsilon_{l,k}$ is the standard location, μ_{zl} and σ_{zl} are the mean and standard deviation of the variable z_l. The standard location $\varepsilon_{l,k}$ and weight $\omega_{l,k}$ are obtained by Hong's method [20]

$$\begin{aligned} \varepsilon_{l,k} &= \frac{\lambda_{l,3}}{2} + (-1)^{3-k}\sqrt{\lambda_{l,4} - \frac{3\lambda_{l,3}^2}{4}} \quad k = 1,2 \\ \varepsilon_{l,3} &= 0 \qquad\qquad\qquad\qquad\quad k = 3 \end{aligned} \tag{31}$$

$$\omega_{l,k} = \frac{(-1)^{3-k}}{\varepsilon_{l,k}(\varepsilon_{l,1} - \varepsilon_{l,2})} \qquad k = 1,2$$

$$\omega_{l,3} = \frac{1}{m} - \frac{1}{\lambda_{l,4} - \lambda_{l,3}^2} \qquad k = 3 \tag{32}$$

where $\lambda_{l,3}$ and $\lambda_{l,4}$ are the skewness and kurtosis of variable z_l. In (31), the setting $\varepsilon_{l,3}$=0 yields $z_{l,3}$ =μ_{zl} in (30), thus m of the concentrations are the same as (μ_{z1} , μ_{z2} ,..., μ_{zl} ,... ,μ_{zm}), and the total number of concentrations would reduce from 3m to 2m+1.

In other words, with the help of (30) to (32) the original uncertain vector (z_1 , z_2 ,..., z_l ,... ,z_m) is substituted by a total number of 2m+1 deterministic vectors as concentrations. Afterwards, conventional power flow and transient stability analysis (TSA) are conducted at each concentration to calculate the concerned outputs, for example the slack bus generation, the reactive power of each generator, node voltages, transmission line power flows and the transient stability margin η. Based on these outputs with their weighting factors, the statistical information of uncertain outputs, such as the raw moment, central moment and the cumulant (hereinafter indicated by (34), (36) and (37)), could be calculated for producing the cumulative distribution functions (CDFs) of uncertain outputs using the Gram-Charlier expansion theory [18] as follows.

The relationship between the concerned outputs S and the concentration (μ_{z1} , μ_{z2},..., $\mu_{z(l-1)}$, $z_{l,k}$, $\mu_{z(l+1)}$,..., μ_{zm}) is denoted by function F as

$$S_{l,k} = F(\mu_{z1}, \mu_{z2},..., \mu_{z(l-1)}, z_{l,k}, \mu_{z(l+1)},..., \mu_{zm}) \tag{33}$$

Then, by using $S_{l,k}$ with its weights $\omega_{l,k}$, the j^{th} raw moment m_j of outputs S is calculated as [18]

$$\begin{aligned} m_j = E(S^j) &= \sum_{l=1}^{m}\sum_{k=1}^{3} \omega_{l,k} \cdot (S_{l,k})^j = \sum_{l=1}^{m}\sum_{k=1}^{2} \omega_{l,k} \cdot (S_{l,k})^j \\ &+ \sum_{l=1}^{m} \omega_{l,3} \cdot [F(\mu_{z1}, \mu_{z2}, \ldots, \mu_{zl}, \ldots, \mu_{zm})]^j \end{aligned} \tag{34}$$

With the various order of raw moments of outputs S, the outputs' CDFs F(x) can be estimated by (35) using the Gram-Charlier expansion [18].

$$\begin{aligned} F(x) = \int_{-\infty}^{\tilde{x}} N(u)du - N(\tilde{x})[&\frac{K_3}{3!\sigma^3}(\tilde{x}^2 - 1) \\ &+ \frac{K_4}{4!\sigma^4}(\tilde{x}^3 - 3\tilde{x}) + \frac{K_5}{5!\sigma^5}(\tilde{x}^4 - 6\tilde{x}^2 + 3)] \end{aligned} \tag{35}$$

where $\tilde{x} = (x - \mu)/\sigma$ is the standardized variable, μ and σ are the mean value and the standard deviation of S; N(*) is the standard normal distribution function; K_j are the j^{th} cumulant of S derived from the central moment M_j as

$$K_3 = M_3,\ K_4 = M_4 - 3(M_2)^2,\ K_5 = M_5 - 10M_3M_2 \tag{36}$$

where j^{th} order central moment M_j is calculated from m_j in (34)

$$\begin{aligned} M_2 &= m_2 - (m_1)^2 \\ M_3 &= m_3 - 3m_1m_2 + 2(m_1)^3 \\ M_4 &= m_4 - 4m_1m_3 + 6(m_1)^2m_2 - 3(m_1)^4 \\ M_5 &= m_5 - 5m_1m_4 + 10(m_1)^2m_3 - 10(m_1)^3m_2 + 4(m_1)^5 \end{aligned} \tag{37}$$

Once the CDFs for the random outputs, including the generation of slack bus generator, reactive powers of all generators, node voltages, transmission line power flows, stability margin, etc., are obtained by (35), the probabilistic constraints in (12)-(14), (29) and the system total fuel cost expectation (10) could be easily evaluated from the CDFs.

As mentioned in Section III.A, random variables are often correlated with each other and these correlations should be taken into account in the probabilistic analysis. The Cholesky decomposition in [46] is adopted here to handle the correlated uncertainties in P-TSCOPF as follows: the correlated input variables are first converted to uncorrelated variables by Cholesky decomposition; then the concentrations $\boldsymbol{A}$ for these uncorrelated variables are worked out and inversed to find the concentrations $\boldsymbol{B}$ for the original correlated input variables. The details of Cholesky decomposition could be found in [46].

Afterwards, the deterministic transient stability analysis is conducted on concentrations $\boldsymbol{B}$ to obtain the CDFs of the random outputs by the 2m+1 PE method as normal.

B. Group search optimization (GSO) with PE approach

GSO is an effective global optimization method based on the producer-scrounger model, and it is initialized with random individuals and approaches the optimal solution by updating the positions of its producer, scroungers and rangers [47]. Recently, an improved GSO has been proposed in [48] and successfully applied to solve discontinuous non-convex TSCOPF problems with complex system model, and this improved GSO method is also adopted as the optimization engine for solving the proposed P-TSCOPF model here.

As the power flow equality constraints (11) and DAEs for traditional and wind generators (15)-(23) are implicitly handled by the deterministic power flow and transient stability simulation embedded within the 2m+1 PE method, only the remaining constraints consisting of the probabilistic inequality constraints (12)-(14) and (29) need to be further handled. Here the penalty function method [49] is adopted to deal with these probabilistic constraints and results in an unconstrained optimization problem like (38) such that it could be readily optimized using the GSO method.

$$\begin{aligned} Min\ F(x,u) = F_G + p_j \max(0, \beta_j - P\{h_j(\mathbf{x}^{t_0}, \mathbf{y}^{t_0}, \mathbf{u}, \boldsymbol{\varepsilon})\}) \\ + p_r \max(0, \beta_r - P\{\eta(\mathbf{x}(t), \mathbf{y}(t), \mathbf{u}, \boldsymbol{\varepsilon})) \end{aligned} \quad (38)$$

where p_j and p_r are the penalty factors to produce large discrimination if any probabilistic constraints in (12)-(14) or (29) are violated.

The main procedures of the proposed GSO-PE method for solving the P-TSCOPF problem are outlined below and depicted in Fig.4.

a) Input system data, generate concentrations for uncertainties in P-TSCOPF model using 2m+1 PE with Cholesky decomposition strategy, and specify GSO parameters and randomly initialize the GSO particles for control variables within the lower and upper limits; (Corresponding to Step (1) to (4) in Fig.4)
b) The CDFs of steady-state variables in (12)-(14), the stability margin in (29) and fuel cost in (10) are calculated based on the results of 2m+1 deterministic TSA by (35), then these probabilistic constraints and fuel cost expectation can be evaluated from the corresponding CDFs; (Corresponding to Step (5) to (8) in Fig.4)
c) Evaluate the fitness of each particle by (38); (Corresponding to Step (9))
d) Find the best fitness among all particles, and determine whether the maximum number of iterations is reached, if yes, output the optimal solutions of P-TSCOPF model; otherwise, increase iteration number and update positions of GSO particles for control variables, then go to phase *b)*; (Corresponding to Step (10) and (11) in Fig.4)

As shown in the flowchart in Fig.4, the proposed GSO-PE is a two-stage algorithm consisting of calculating the probabilistic outputs by 2m+1 PE strategy from step (5) to (8) and updating control variable by GSO in the outer loop. Since SIME conducted transient stability analysis based on time domain simulation, it has good adaptability to complex dynamic models for transient stability study. The core of GSO-PE algorithm is to transform the PTSA into a set of deterministic transient stability analysis conducted by SIME. The propose GSO-PE is therefore very flexible and expandable to solve a P-TSCOPF model with any types of renewables and dynamic models.

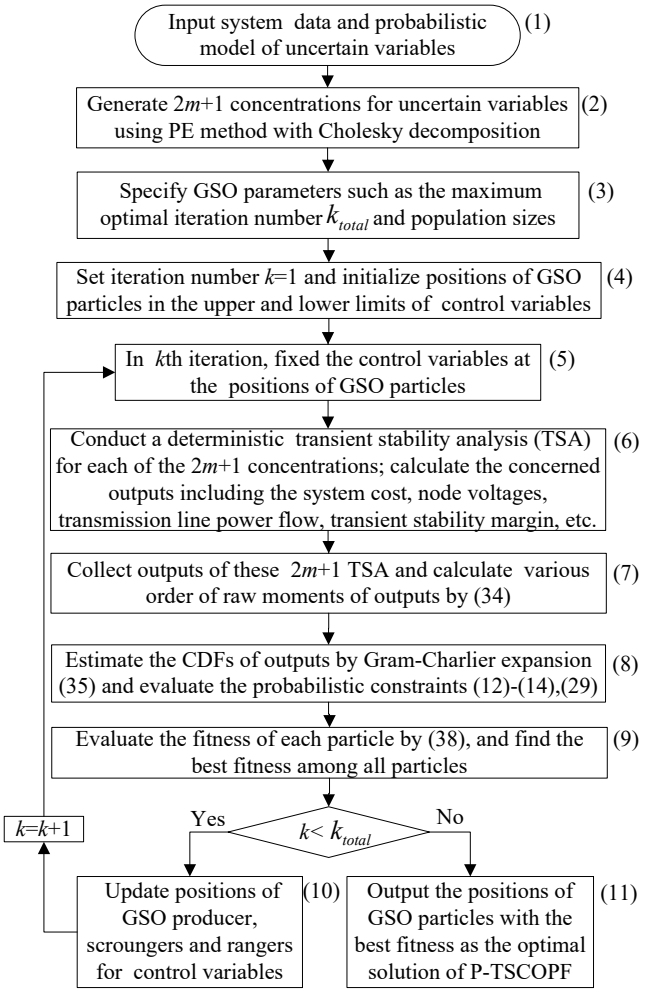

Fig. 4 Flowchart of GSO-PE for solving P-TSCOPF model

V. CASE STUDY

For evaluating the proposed P-TSCOPF model and GSO-PE approach, a modified New England 39-bus system with four correlated wind farms (WFs) as shown in Fig. 5 is prepared. The fuel cost coefficients of generators at bus 30 to 39 are cited from [28], and their dynamic models for transient stability analysis are 4th order model equipped with IEEE Type 1 exciter as listed in Table 1. For WFs, an aggregated model is sufficient for investigating its impact on the system transient stability [50]. Specifically, a total number of 100 DFIGs with rated power 2 MW each cited from [40] are aggregated to form a WF with wind turbine parameters: K_{tw}=0.6p.u./rad, D_{tw}=0.45 and H_t=3.8s.

The contingency considered in transient stability analysis is a three-phase earth fault occurred at one end of line 15-16 near bus 15 at t=0ms, and subsequently cleared by tripping line 15-16 after a time period t_{cl}. The transient stability analysis is conducted for 10s with integration step of 0.01s by running an in-house program under MATLAB R2010b. Generator reactive power limits and transmission line thermal limits are cited from Matpower [51]; the node voltages of PQ bus are

required to be in the range [0.97, 1.06]. The threshold of all probabilistic constraints (i.e. β_Q, β_V, β_S, and β_r) are assumed as 0.95, which means when all the left parts of the probabilistic constraints (12)-(14) and (29) are not smaller than 0.95, the corresponding operation point is considered as acceptable in the view of security risk.

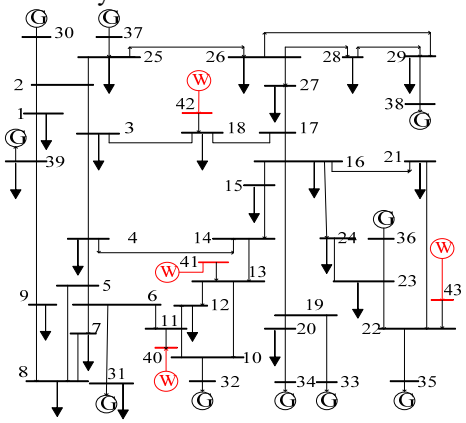

Fig. 5 Modified New England System with four WFs

Table 1 IEEE Type 1 Exciter Parameters for New England system

K_A	T_A (s)	K_E	T_E (s)	K_F	T_F (s)	A_{ex}	B_{ex}	V_{rmin}	V_{rmax}
20	0.055	0.36	0.05	0.125	1.8	0.0056	1.075	-10	10

The following are the uncertain parameter settings for the random input variables.

1) The base load given in [51] is assumed as the mean value of the normal distributed load injection with the standard deviation fixed as 10% of the mean value. There are totally 21 correlated loads with correlations assumed as 0.15.
2) The shape and scale parameters of wind speed are set as λ=2 and k=12 with correlations of 0.3, while the cut-in, cut-out and rated wind speed for WTs are v_{ci}=3m/s, v_{ct}=25m/s and v_{rd}=12 m/s [52], respectively.
3) The parameters for the normal distribution fault clearing time are set as μ_t =350ms, σ_t =0.1μ_t.

A. *Benchmarking and comparison of results*

For evaluating the accuracy and efficiency of the proposed GSO-PE method, the widely used MC method is deployed for benchmarking. Both the MC and GSO-PE methods run on a PC with a 3.0GHz Intel Core2Quad CPU and 4GB RAM. The required number of samples of MC is estimated as 5,000 based on the convergence theory [53]. The performance of GSO-PE is compared with MC using the mean and standard deviation (SD) error ε_μ^x and ε_σ^x as

$$\varepsilon_\mu^x = 100(|\mu_{MC} - \mu_{PE}|)/\mu_{MC}[\%] \quad (39)$$

$$\varepsilon_\sigma^x = 100(|\sigma_{MC} - \sigma_{PE}|)/\sigma_{MC}[\%] \quad (40)$$

where μ_{MC}, σ_{MC}, μ_{PE} and σ_{PE} are the mean value and standard deviation of output random variables calculated by MC and GSO-PE method, respectively. The Average Root Mean Square (ARMS) [18] error of output random variables resulting from the GSO-PE method is measured by an accuracy index as

$$\text{ARMS} = \frac{\sqrt{\sum_{i=1}^{N}(F_{MC_i} - F_{PE_i})^2}}{N} \quad (41)$$

where F_{MCi} and F_{PEi} are the values on the CDF curve solved by MC and GSO-PE method, respectively. N is the number of selected points chosen from its CDF curve. Here, N is set as 10 for the range of CDF curve with confident level [2%, 98%].

B. *Investigations on the base case*

The proposed P-TSCOPF model is first checked on the base case with original generations and slack bus voltage cited from [54] and shown in Table 2.

Table 2 Base case and P-TSCOPF solutions (on 100MW base)

Control Variables	Base case	P-TSCOPF solution
G_{30}(p.u.)	2.5	2.81
G_{32}(p.u.)	6.5	4.76
G_{33}(p.u.)	6.32	6.52
G_{34}(p.u.)	5.08	5.36
G_{35}(p.u.)	6.5	4.11
G_{36}(p.u.)	5.6	2.41
G_{37}(p.u.)	5.4	4.85
G_{38}(p.u.)	8.3	8.69
G_{39}(p.u.)	10	11.99
V_{31}(p.u.)	0.982	1.095
All Constraints Satisfied	No	Yes
Cost Expectation ($/h)	57,486.97	59,008.96
CPU Time (s)	24	2,647

For illustrating how the system dynamics in the base case is analyzed using SIME, one typical concentration (μ_{z1} , μ_{z2} ,..., μ_{zl} , ... ,μ_{zm}) is generated for the uncertain factors by PE using (30) with $\varepsilon_{l,3}$=0. This concentration is a vector consisting of the mean values of all uncertain factors. With this concentration and the base case, conventional power flow and time domain simulations are conducted to calculate the transient stability margin. A set of curves including 10 generator angles, OMIB mechanical and electric power, and OMIB kinetic energy, is provided in Fig.6 where Fig.6a shows the England system is unstable for the sampled point, in which Generator 1 to Generator 9 are CMs and Generator 10 is NMs, Fig.6b indicates the unstable condition (26) satisfied at 0.752s as the instability time, and Fig.6c demonstrates the kinetic energy at 0.752s is with a minimal value as 5.514 pu-rad. According to (25), the transient stability margin is -5.514 pu-rad as the negative of the minimal kinetic energy.

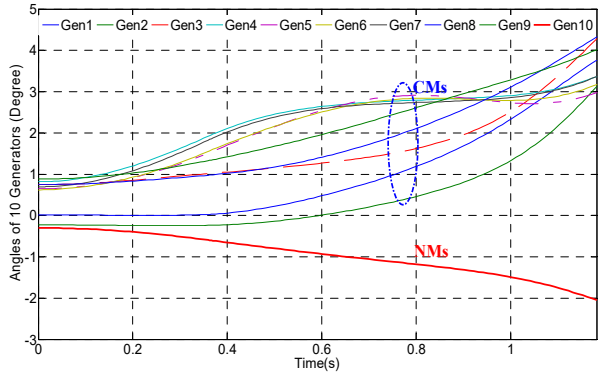

(a) Angle curves of 10 generators

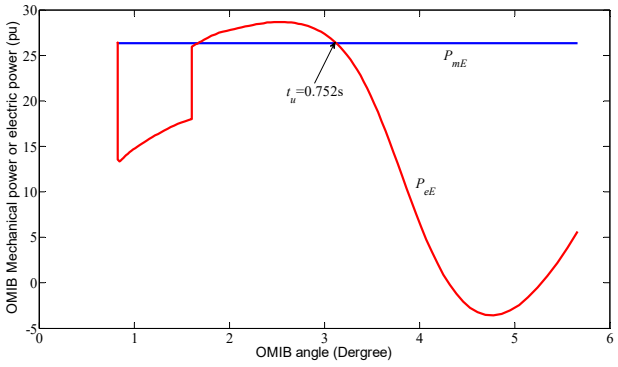

(b) OMIB mechanical power and electric power

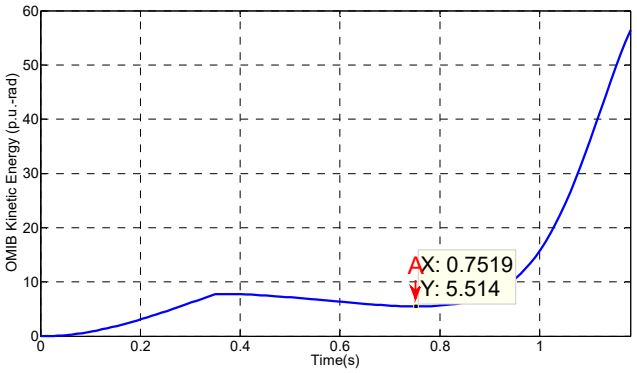

(c) OMIB kinetic energy curve of whole power system

Fig.6 Stability analysis for a concentration generated by PE

For other concentrations generated by PE or MC method, the deterministic power flow and time domain simulation are repeated similarly to determine the outputs concerned, and then all these results with their weighting factors are collected to estimate the CDFs and evaluate the probabilistic constraints.

For the base case, the CDF of generator output at slack bus analyzed by the PE method is shown in Fig.7, and the expectation of England system total fuel cost is relatively low as 57,486.97 $/h. However, at this operating point, not all the probabilistic constraints are satisfied with the acceptable risk security level. For example, based on the CDF profile in Fig. 8, the probability of voltage for bus 4 in range [0.97, 1.06] is only 0.19, which is calculated by subtracting the probability at point A from 1. This indicates the probabilistic voltage constraint (13) cannot be fulfilled with the required 0.95 security level. Similarly, the probabilistic constraint for transmission line 6-11 is also violated as shown in Fig. 9. With its thermal limit being 6 p.u., the probability at point B is 0.498 which indicates the probability of power flow lower than 6 p.u. is 0.498 for line 6-11. In other words, the probability of over-loading line 6-11 is 0.502, which considerably violates the limit that probability of line over-loading shall not be larger than 1-0.95=0.05. Moreover, the probabilistic transient stability margin for stable case (stability margin $\eta>0$, on the right of Point C) is 0.522 as shown in Fig. 10, which indicates that the system would lose transient stability with a probability of 0.478; therefore, the system cannot maintain the transient stability with a satisfactory security level.

The MC method with 5,000 samples is also conducted for benchmarking the performance of the $2m+1$ PE method. The total computation time taken by the MC method is 2,236s, which is almost 2 orders of magnitude slower than the proposed $2m+1$ PE method whose computation time is only 24s. Compared with the large number of time domain simulations required by the MC method, the $2m+1$ PE method only needs to perform a small fraction of time domain simulations and is therefore significantly more efficient. For instance, only 53 time domain simulations would be needed with $m=26$ as in this case study. Furthermore, the accuracy of the PE method is diligently validated by qualitatively comparing the probability curves of slack bus generation (P_{slack}), voltage in bus 4 (V_4), power flow in line 6-11 ($P_{6\text{-}11}$), and transient stability margin (SM) obtained by the PE and MC methods as plotted in Fig. 7-10. The results of this comparison study are concisely summarized in Table 3. As is evidenced by the small mean and SD errors (<10.3% and <6.8%, respectively) as well as small ARMS errors (<0.2%) found in all the four variables in concern, the accuracy of the PE method is acceptable for its application in P-TSCOPF.

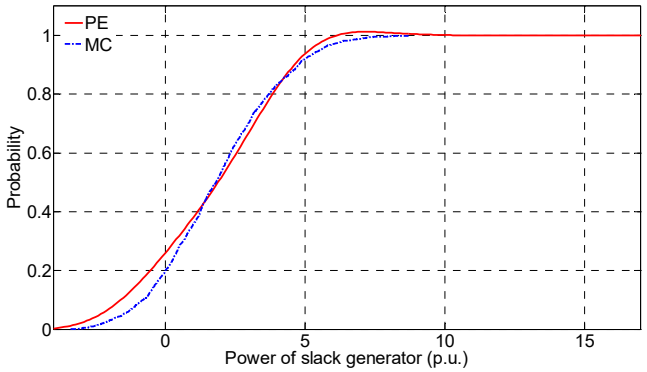

Fig. 7 Probabilistic generation at slack bus

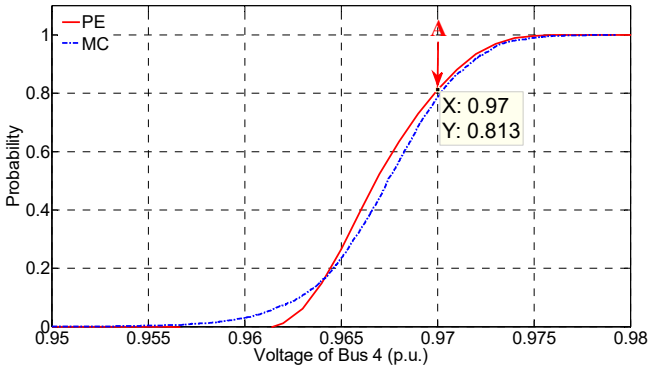

Fig. 8 Probabilistic voltage in bus 4

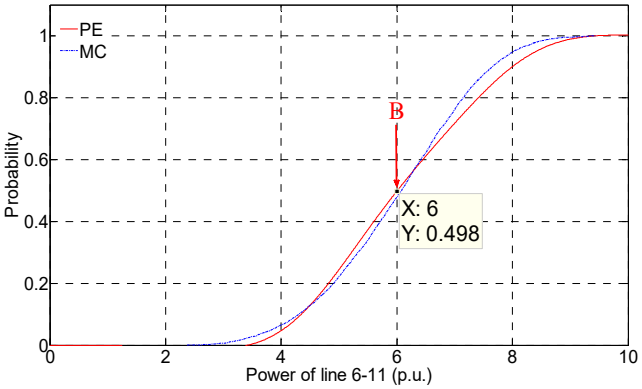

Fig. 9 Probabilistic power flow in line 6-11

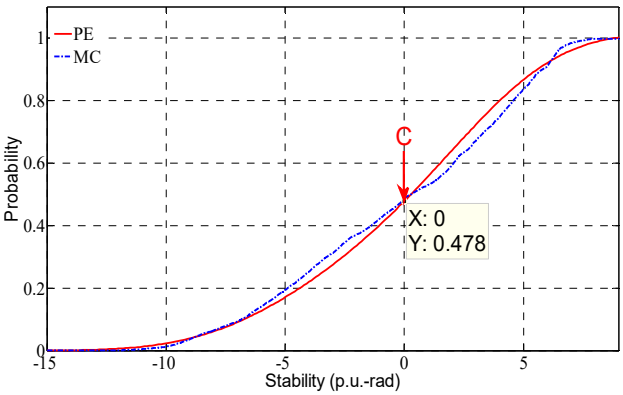

Fig. 10 Probabilistic stability margin

Table 3 Error comparisons for the base case

Variable	MC (Mean, SD)	PE (Mean, SD)	Error (%)		
			ε_μ^x	ε_σ^x	ARMS
V_4	(0.9686,0.0012)	(0.9684,0.0013)	0.02	3.63	0.19
$P_{6\text{-}11}$	(5.9911,1.0510)	(6.1421,1.0799)	2.52	2.76	0.10
SM	(-0.1594,4.8406)	(-0.1758,4.5155)	10.28	6.72	0.09
P_{slack}	(1.7826,2.1355)	(1.6453,2.2283)	7.70	4.35	0.15
CPU time (s)	2236	24	Speed Ratio 2236/24=93.2		

C. *Investigations on the optimal solution of P-TSCOPF model*

As shown in previous section, the base case does pose a high risk of system instability. A new operating point, which shall be secure and economic, is therefore desirable and can be found using the proposed GSO-PE method as demonstrated in the following case study, which contains 10 control variables consisting of 9 generator active powers and the slack bus voltage in the range of [0.95, 1.1]. The population size of GSO-PE is 15 and the number of total iterations is fixed at 30. Parameters for initializing GSO-PE individuals are cited from [48]. The penalty factors p_j and p_r in (38) are set to 10^7 so as to introduce sufficient discriminations for any constraint violations in the P-TSCOPF model.

Fig. 11 plots the convergence of the proposed GSO-PE optimization applied to solve this P-TSCOPF problem. The convergence is good and the total CPU time taken for the whole optimization process is 2,647s which is comparable to a single run of MC for assessing the base case in section V.B.

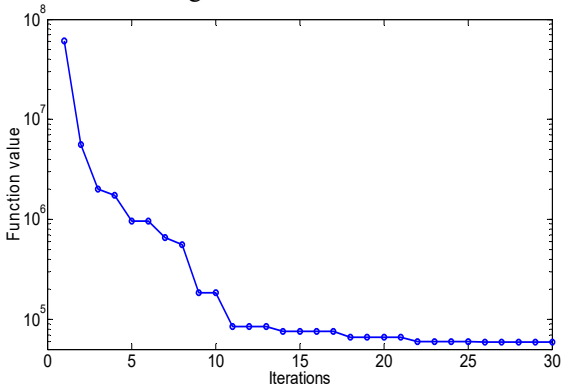

Fig. 11 Convergence of GSO-PE approach for New England system

After this P-TSCOPF optimization, the system has a slightly higher total fuel cost expectation of 59,008.96 $/h, which is increased by 2.6% compared to the base case as a small price to pay to mitigate the risk of instability. The optimized solution given in Table 2 is probabilistically transient stable and all the probabilistic static constraints are satisfied. For example, as shown in Fig.12, the probability at Point A on the CDF curve of bus 4 voltage is 0.006, thus the probability of voltage in the range of [0.97, 1.06] is 0.994 which is higher than the required security level 0.95. In Fig.13, the probability of line flow 6-11 below the thermal limit 6 p.u. at Point B is 0.96 which is also higher than the required risk security level 0.95. In other words, this line is statistically unlikely to be overloaded. Moreover, the probability plot of stability margin in Fig.14 indicates that the system is stable (stability margin η>0, on the right of Point C) with a high probability near 1 even with the given uncertainties. Meanwhile, the probability curves of bus 4 voltage, power flow of line 6-11 and transient stability margin obtained using the MC method are also given in Fig. 12-14 to show the good match of results between the PE and MC methods.

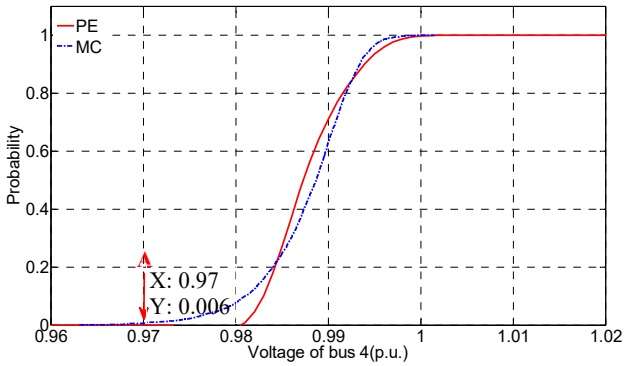

Fig. 12 Voltage probability of bus 4

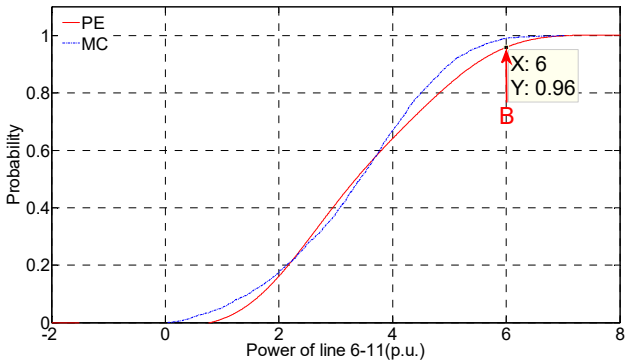

Fig. 13 Power probability of line 6-11

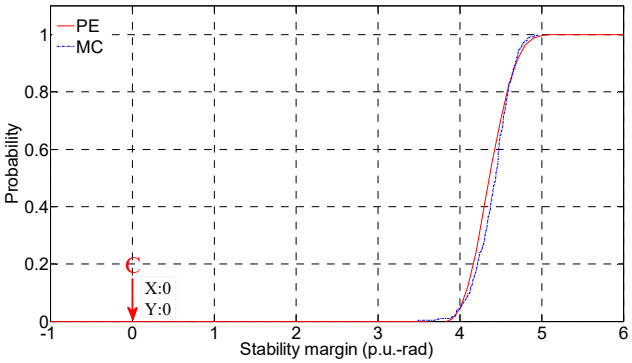

Fig. 14 Probability of stability margin

Table 4 checks the accuracy and effectiveness of the solution found by the proposed GSO-PE method with the MC method. Again, as the mean, SD, and ARMS errors are small (<2.8%, <4.8%, and <0.6%, respectively), the GSO-PE method can be used as the fast alterative of the MC method with acceptable accuracy, and GSO-PE indeed approached an optimal solution for effectively enhancing the probabilistic security level.

Table 4 Error comparisons for optimal solution

Variable	MC (Mean, SD)	GSO-PE (Mean, SD)	Error (%)		
			ε_μ^x	ε_σ^x	ARMS
V_4	(0.9876,0.0042)	(0.9880,0.0040)	0.04	4.76	0.45
$P_{6\text{-}11}$	(3.4174,1.3011)	(3.5041,1.3485)	2.53	3.64	0.15
SM	(4.4237,0.2289)	(4.3737,0.2271)	1.13	0.78	0.60
P_{slack}	(6.5295,3.4782)	(6.3513,3.5012)	2.73	0.66	0.16

The fuel cost expectations at different security levels for β_Q, β_V, β_S, and β_r are also investigated. As shown in Table 5, the fuel cost expectation is relative small when the security level is low.

With a higher security level, the fuel cost expectation increased as expected since the system has to pay a higher expected fuel cost to establish a more secure operation state. Results presented in Table 5 also provide qualitative information to power system operators for making decisions in selecting the best compromised operation point with low expected fuel cost and acceptable system security level.

Table 5 Fuel cost expectations at different security levels

Confident Level	0.80	0.85	0.90	0.95	0.98
Fuel Cost($/h)	57189	57420	57876	59009	59885

REMARKS:

1. The solution speed of the proposed GSO-PE method could be substantially further improved by exploring its inherent parallelism to run on a high-performance computer cluster. Since samples are independent of each other, its parallel computation efficiency will be expected to be very high and the proposed P-TSCOPF model could be applied to practical power systems for on-line dynamic security constrained preventive control.
2. In terms of modeling, the proposed P-TSCOPF model is highly adaptable and flexible, and could be easily extended to include dynamic models of any intermittent generations or uncertain renewables such as photovoltaic power generations, electric vehicle aggregators, etc.

VI. CONCLUSIONS

In this paper, a probabilistic transient stability constrained optimal power flow (P-TSCOPF) problem is investigated for power system preventive control so as to enhance the probabilistic transient stability security. While a very general P-TSCOPF model has first been put forward, a specific one simultaneously considering the transient stability and uncertainties stemming from the correlated uncertain loads, uncertain fault clearing time and multiple correlated wind generations, etc. was then established. A hybrid GSO-PE solution approach based on the point-estimated method and group search optimization algorithm was thus proposed to efficiently solve this challenging P-TSCOPF model. Tests and analysis on the modified New England 39-bus system with four correlated uncertain WFs have demonstrated the validity of the P-TSCOPF model for improving the probabilistic security level and the effectiveness of GSO-PE method. Compared with the widely used MC method, the proposed GSO-PE method is orders of magnitude faster while the solution quality is generally comparable. Further acceleration on the solution speed and support for other dynamic models of intermittent generations or uncertain renewables have also been discussed.

REFERENCES

[1] Y. Chen, J. Y. Wen, and S. J. Cheng, "Probabilistic Load Flow Method Based on Nataf Transformation and Latin Hypercube Sampling," *IEEE Trans. Sustainable Energy,* vol. 4, no. 2, pp. 294-301, Apr. 2013.

[2] N. Soleimanpour and M. Mohammadi, "Probabilistic Load Flow by Using Nonparametric Density Estimators," *IEEE Trans. Power Syst.,* vol. 28, no. 4, pp. 3747-3755, Nov. 2013.

[3] F. J. Ruiz-Rodriguez, J. C. Hernández, and F. Jurado, "Probabilistic load flow for photovoltaic distributed generation using the Cornish–Fisher expansion," *Electric Power Syst. Research,* vol. 89, pp. 129-138, Aug. 2012.

[4] H. Zhang and P. Li, "Probabilistic analysis for optimal power flow under uncertainty," *Generation, Transmission & Distribution, IET,* vol. 4, no. 5, pp. 553-561, May 2010.

[5] X. Li, Y. Z. Li, and S. H. Zhang, "Analysis of Probabilistic Optimal Power Flow Taking Account of the Variation of Load Power," *IEEE Trans. Power Syst.,* vol. 23, no. 3, pp. 992-999, Aug. 2008.

[6] H. Zhang and P. Li, "Chance constrained programming for optimal power flow under uncertainty," *IEEE Trans. Power Syst.,* vol. 26, no. 4, pp. 2417-2424, Nov. 2011.

[7] H. Yu, C. Y. Chung, and K. P. Wong, et al., "A chance constrained transmission network expansion planning method with consideration of load and wind farm uncertainties," *IEEE Trans. Power Syst.,* vol. 24, no. 3, pp. 1568-1576, Aug. 2009.

[8] R. Billinton and P. R. S. Kuruganty, "Probabilistic assessment of transient stability in a practical multimachine system," *IEEE Trans. Power Appar. Syst.,* vol. PAS-100, no. 7, pp. 3634-3641, Jul. 1981.

[9] R. Billinton and P. R. S. Kuruganty, "A probabilistic index for transient stability," *IEEE Trans. Power Appar. Syst.,* vol. PAS-99, no. 1, pp. 195-206, Jan. 1980.

[10] P. M. Anderson and A. Bose, "A probabilistic approach to power system stability analysis," *IEEE Trans. Power Appar. Syst.,* vol. PAS-102, no. 8, pp. 2430-2439, Aug. 1983.

[11] E. Chiodo, F. Gagliardi, and D. Lauria, "Probabilistic approach to transient stability evaluation," *IEE Proc.-Gener., Transm. and Distrib.,* vol. 141, no. 5, pp. 537-544, Sep. 1994.

[12] E. Chiodo and D. Lauria, "Transient stability evaluation of multimachine power systems: a probabilistic approach based upon the extended equal area criterion," *IEE Proc.-Gener., Transm. and Distrib.,* vol. 141, no. 6, pp. 545-553, Nov. 1994.

[13] E. Chiodo, F. Gagliardi, and M. La Scala, et al., "Probabilistic on-line transient stability analysis," *IEE Proc.-Gener., Transm. and Distrib.,* vol. 146, no. 2, pp. 176-180, Mar. 1999.

[14] R. Billinton and S. Aboreshaid, "Stochastic modelling of high-speed reclosing in probabilistic transient stability studies," *IEE Proc.-Gener., Transm. and Distrib.,* vol. 142, no. 4, pp. 350-354, Jul. 1995.

[15] J. D. McCalley, A. A. Fouad, and V. Vittal, et al., "A risk-based security index for determining operating limits in stability-limited electric power systems," *IEEE Trans. Power Syst.,* vol. 12, no. 3, pp. 1210-1219, Aug. 1997.

[16] D. Z. Fang, L. Jing, and T. S. Chung, "Corrected transient energy function-based strategy for stability probability assessment of power systems," *IET Gener., Transm. & Distrib.,* vol. 2, no. 3, pp. 424-432, May 2008.

[17] S. O. Faried, R. Billinton, and S. Aboreshaid, "Probabilistic evaluation of transient stability of a wind farm," *IEEE Trans. Energy Conversion,* vol. 24, no. 3, pp. 733-739, Sep. 2009.

[18] P. Zhang and S. T. Lee, "Probabilistic load flow computation using the method of combined cumulants and Gram-Charlier expansion," *IEEE Trans. Power Syst.,* vol. 19, no. 1, pp. 676-682, Feb. 2004.

[19] D. Villanueva, J. L. Pazos, and A. Feijoo, "Probabilistic load flow including wind power generation," *IEEE Trans. Power Syst.,* vol. 26, no. 3, pp. 1659-1667, Aug. 2011.

[20] H. P. Hong, "An efficient point estimate method for probabilistic analysis," *Reliability Engineering and System Safety,* vol. 59, no. 3, pp. 261-267, 1998.

[21] J. M. Morales and J. Perez-Ruiz, "Point estimate schemes to solve the probabilistic power flow," *IEEE Trans. Power Syst.,* vol. 22, no. 4, pp. 1594-1601, Nov. 2007.

[22] X. H. Yan and V. H. Quintana, "An efficient predictor-corrector interior point algorithm for security-constrained economic dispatch," *IEEE Trans. Power Syst.,* vol. 12, no. 2, pp. 803-810, May 1997.

[23] Y. Fu, M. Shahidehpour, and Z. Y. Li, "Security-constrained unit commitment with AC constraints," *IEEE Trans. Power Syst.,* vol. 20, no. 2, pp. 1001- 1013, May 2005.

[24] Y. Fu and M. Shahidehpour, "Fast SCUC for Large-Scale Power Systems," *IEEE Trans. Power Syst.,* vol. 22, no. 4, pp. 2144-2151, Nov. 2007.

[25] Y. Xu, Z. Y. Dong, and R. Zhang, et al., "A Decomposition-Based Practical Approach to Transient Stability-Constrained Unit Commitment," *IEEE Trans. Power Syst.,* vol. 30, no. 3, pp. 1455-1464, May 2015.

[26] Q. Jiang, B. Zhou, and M. Zhang, "Parallel Augment Lagrangian Relaxation method for transient stability constrained unit commitment," *IEEE Trans. Power Syst.,* vol. 28, no. 2, pp. 1140-1148, May 2013.

[27] K. S. Chandrashekhar and D. J. Hill, "Dynamic Security Dispatch: Basic Formulation," *IEEE Trans. Power Appar. Syst.,* vol. PAS-102, no. 7, pp. 2145-2154, Jul. 1983.

[28] T. B. Nguyen and M. A. Pai, "Dynamic security-constrained rescheduling of power systems using trajectory sensitivities," *IEEE Trans. Power Syst.,* vol. 18, no. 2, pp. 848- 854, May 2003.
[29] H. Yu, C. Y. Chung, and K. P. Wong, et al., "Probabilistic Load Flow Evaluation With Hybrid Latin Hypercube Sampling and Cholesky Decomposition," *IEEE Trans. on Power Syst.,* vol. 24, no. 2, pp. 661-667, May 2009.
[30] D. Villanueva, A. E. Feijóo, and J. L. Pazos, "An analytical method to solve the probabilistic load flow considering load demand correlation using the DC load flow," *Electric Power Syst. Research,* vol. 110, pp. 1-8, May 2014.
[31] M. Hajian, W. D. Rosehart, and H. Zareipour, "Probabilistic power flow by Monte Carlo simulation with Latin supercube sampling,", *IEEE Trans. Power Syst.,* vol. 28, no. 2, pp. 1550-1559, May 2013.
[32] A. Dissanayaka, U. D. Annakkage, and B. Jayasekara, et al., "Risk-Based Dynamic Security Assessment," *IEEE Trans. Power Syst.,* vol. 26, no. 3, pp. 1302-1308, Aug. 2011.
[33] M. Ali, Z. Y. Dong, and P. Zhang, et al., "Probabilistic Transient Stability Analysis using Grid Computing Technology," in *Proc. IEEE Power Engineering Society General Meeting*, 2007, pp. 1-7.
[34] H. Huang, C. Y. Chung, and K. W. Chan, et al., "Quasi-Monte Carlo Based Probabilistic Small Signal Stability Analysis for Power Systems With Plug-In Electric Vehicle and Wind Power Integration," *IEEE Trans. Power Syst.,* vol. 28, no. 3, pp. 3335-3343, Aug. 2013.
[35] H. Huang and C. Y. Chung, "Coordinated damping control design for DFIG-based wind generation considering power output variation," *IEEE Trans. Power Syst.,* vol. 27, no. 4, pp. 1916-1925, Nov. 2012.
[36] W. Wangdee and R. Billinton, "Considering load-carrying capability and wind speed correlation of WECS in generation adequacy assessment," *IEEE Trans. Energy Conversion,* vol. 21, no. 3, pp. 734-741, Sep. 2006.
[37] A. Feijóo, D. Villanueva, and J. L. Pazos, et al., "Simulation of correlated wind speeds: A review," *Renewable and Sustainable Energy Reviews,* vol. 15, no. 6, pp. 2826-2832, Aug. 2011.
[38] D. A. Bechrakis and P. D. Sparis, "Correlation of wind speed between neighboring measuring stations," *IEEE Trans. Energy Conversion,* vol. 19, no. 2, pp. 400-406, Jun. 2004.
[39] P. W. Sauer and M. A. Pai, *Power system dynamics and stability*. Englewood Cliffs, NJ: Prentice-Hall, 1998.
[40] O. Anaya-lara, N. Jenkins, and J. Ekanayake, et al., *wind energy generation modelling and control*. West Sussex: A john Wiley and Sons, Ltd., 2009.
[41] M. Pavella, D. Ernst, and D. Ruiz-Vega, *Transient stability of power systems: a unified approach to assessment and control*. Norwell, MA: Kluwer, 2000.
[42] D. Ernst, D. Ruiz-Vega, and M. Pavella, et al., "A unified approach to transient stability contingency filtering, ranking and assessment," *IEEE Trans. Power Syst.,* vol. 16, no. 3, pp. 435-443, Aug. 2001.
[43] Y. Zhang, L. Wehenkel, and P. Rousseaux, et al., "SIME: A hybrid approach to fast transient stability assessment and contingency selection," *International Journal of Electrical Power & Energy Systems,* vol. 19, no. 3, pp. 195-208, Mar. 1997.
[44] A. Pizano-Martinez, C. R. Fuerte-Esquivel, and D. Ruiz-Vega, "A new practical approach to transient stability-constrained optimal power flow," *IEEE Trans. Power Syst.,* vol. 26, no. 3, pp. 1686-1696, Aug. 2011.
[45] A. Pizano-Martianez, C. R. Fuerte-Esquivel, and D. Ruiz-Vega, "Global transient stability-constrained optimal power flow using an OMIB reference trajectory," *IEEE Trans. Power Syst.,* vol. 25, no. 1, pp. 392-403, Feb. 2010.
[46] J. M. Morales, L. Baringo, and A. J. Conejo, et al., "Probabilistic power flow with correlated wind sources," *IET Gener. Transm. & Distrib.,* vol. 4, no. 5, pp. 641-651, May 2010.
[47] S. He, Q. H. Wu, and J. R. Saunders, "Group Search Optimizer: an optimization algorithm inspired by animal searching behavior," *IEEE Trans. Evol. Comput.,* vol. 13, no. 5, pp. 973-990, Oct. 2009.
[48] S. W. Xia, B. Zhou, and K. W. Chan, et al., "An improved GSO method for discontinuous non-convex transient stability constrained optimal power flow with complex system model," *International Journal of Electrical Power & Energy Systems,* vol. 64, pp. 483-492, Jan. 2015.
[49] N. Mo, Z. Y. Zou, and K. W. Chan, et al., "Transient stability constrained optimal power flow using particle swarm optimisation," *IET Gener. Transm. Distrib.,* vol. 1, no. 3, pp. 476-483, May 2007.
[50] D. Gautam, L. Goel, and R. Ayyanar, et al., "Control strategy to mitigate the impact of reduced inertia due to doubly fed induction generators on large power systems," *IEEE Trans. Power Syst.,* vol. 26, no. 1, pp. 214-224, Feb. 2011.
[51] R. D. Zimmerman, C. E. Murillo-Sanchez, and D. Gan, "MATPOWER: a Matlab power system simulation package 2006," *http://www.pserc.cornell.edu//matpower/*.
[52] "GE Power & Water, Renewable Energy," *http://www.ge-energy.com/products_and_services/products/wind_turbines*.
[53] A. M. Leite Da Silva, R. A. G. Fernandez, and C. Singh, "Generating capacity reliability evaluation based on Monte Carlo simulation and Cross-Entropy methods," *IEEE Trans. Power Syst.,* vol. 25, no. 1, pp. 129-137, Feb. 2010.
[54] K. R. Padiyar, *Power system dynamics: stability and control*. Singapore: John Wiley & Sons (Asia) Pte Ltd, 1996.

Shiwei XIA (S'12) received the B.Eng. and M.Eng. degrees in electrical engineering from Harbin Institute of Technology, Harbin, in 2007 and 2009 respectively, and the Ph.D. degree in power systems from The Hong Kong Polytechnic University, Hong Kong, in 2015. Afterwards, he worked as a Research Associate and subsequently as a Postdoctoral Fellow in the Department of Electrical Engineering of The Hong Kong Polytechnic University in 2015. He is currently with the State Key Laboratory of Alternate Electrical Power System with Renewable Energy Sources, School of Electrical & Electronic Engineering, North China Electric Power University, Beijing. His research interests generally include security and risk analysis for power systems with renewable energies, distributed optimization and control of multiple sustainable energy sources in smart grid.

Xiao Luo received the B.Eng. degree (Hons) in electrical engineering from The Hong Kong Polytechnic University, Hong Kong, China, in 2011. He is currently pursuing the Ph.D. degree at the Department of Electrical Engineering in The Hong Kong Polytechnic University. His major research interests include EV charging control, demand response, wind power integration, and power market.

Ka Wing Chan (M'98) received the B.sc. (Hons) and Ph.D. degrees in electronic and electrical engineering from the University of Bath, Bath, U.K., in 1988 and 1992, respectively. He currently is an Associate Professor and Associate Head in the Department of Electrical Engineering of the Hong Kong Polytechnic University. His general research interests include power system stability, analysis, control, security and optimization, real-time simulation of power system transients, distributed and parallel processing, and artificial intelligence techniques.

Ming ZHOU was born in Hubei, China, on October 1967. She received the Ph.D. degree from North China Electric Power University, China, in 2006. She was a visiting scholar in the Department of Electrical and Electronic Engineering, The University of Hong Kong, from 2003-2004. She is currently a Professor in the School of Electrical and Electronic Engineering, North China Electric Power University, Beijing. Her major interests include power system modeling, and power system electricity market with demand response.

Gengyin LI was born in Hebei, China, on May 1964. He received the Ph.D. degree in electric engineering from North China Electric Power University, China, in 1996. He is a Professor and the Executive Dean of the School of Electrical and Electronic Engineering, North China Electric Power University, Beijing. His special fields of interest include power system operation and planning, stability analysis and control of large-scale hybrid AC-DC power systems.